European Journal of Neuroscience, Vol. 21, pp. 611–621, 2005

A role for synGAP in regulating neuronal apoptosis

Irene Knuesel,[1,*] Abigail Elliott,[1] Hong-Jung Chen,[1,†] Isabelle M. Mansuy[2] and Mary B. Kennedy[1]
[1]Division of Biology 216-76, California Institute of Technology, Pasadena, CA 91125, USA
[2]Department of Biology, Swiss Federal Institute of Technology, ETH Hönggerberg HPM D24, CH-8093, Zurich, Switzerland

Keywords: caspase-3, Cre, mouse, postsynaptic density, Ras/Rap1

Abstract

The brain-specific Ras/Rap GTPase-activating protein synGAP is a major component of the postsynaptic density at glutamatergic synapses. It is a target for phosphorylation by Ca^{2+}/calmodulin-dependent protein kinase II, which up-regulates its GTPase-activating activity. Thus, SynGAP may play an important role in coupling *N*-methyl-D-aspartate-type glutamate receptor activation to signaling pathways downstream of Ras or Rap. Homozygous deletion of synGAP is lethal within the first few days after birth. Therefore, to study the functions of synGAP, we used the cre/loxP recombination system to produce conditional mice mutants in which gradual loss of synGAP begins at ~1 week, and usually becomes maximal by 3 weeks, after birth. The resulting phenotypes fall into two groups. In a small group, the level of synGAP protein is reduced to 20–25% of wild type, and they die at 2–3 weeks of age. In a larger group, the levels remain higher than ~40% of wild type, and they survive and remain healthy. In all mutants, however, an abnormally high number of neurons in the hippocampus and cortex undergo apoptosis, as detected by caspase-3 activation. The effect is cell autonomous, occurring only in neuronal types in which the synGAP gene is eliminated. The level of caspase-3 activation in neurons correlates inversely with the level of synGAP protein measured at 2 and 8 weeks after birth, indicating that neuronal apoptosis is enhanced by reduction of synGAP. These data show that synGAP plays a role in regulation of the onset of apoptotic neuronal death.

Introduction

At excitatory postsynaptic terminals of glutamatergic neurons, calcium influx through the *N*-methyl-D-aspartate (NMDA)-type glutamate receptor (NMDA receptor) contributes to the control of a wide variety of neuronal processes, including synaptic plasticity, synapse formation and cell death. A core complex of signaling proteins associated with the NMDA receptor is found in the postsynaptic density (PSD) fraction (Kennedy, 1997, 2000; Sheng & Sala, 2001), and is postulated to relay signals controlled by activation of the NMDA receptor. Among the most prominent proteins in this complex are PSD-95, Ca^{2+}/calmodulin-dependent protein kinase II (CaMKII) and synGAP (Chen *et al*., 1998; Kim *et al*., 1998), a Ras GAP protein also recently shown to possess Rap GAP activity (Krapivinsky *et al*., 2004). In the PSD, synGAP associates with the PSD-95 family and MUPP1 scaffold proteins (Chen *et al*., 1998; Kim *et al*., 1998; Zhang *et al*., 1999; Krapivinsky *et al*., 2004) and is phosphorylated by CaMKII, which increases its GAP activity ~two-fold (Oh *et al*., 2004), potentially decreasing the amount of activated Ras at the synapse. Through this mechanism, synGAP may integrate NMDA receptor activation and Ras signaling pathways and thus influence many neuronal processes.

RasGAPs have previously been implicated in regulation of developmental programs in the brain. Neurons from mice lacking synGAP undergo precocious synapse formation (Vazquez *et al*., 2004). Mice lacking the related protein, p120-RasGAP, show a variety of developmental defects including extensive embryonic neuronal cell death (Henkemeyer *et al*., 1995). These effects may be due, in part, to deregulation of Ras. Ras-dependent pathways have been shown to promote both neuronal cell survival (Kurada & White, 1998; Bonni *et al*., 1999; Mazzoni *et al*., 1999; Botella *et al*., 2003) and cell death (Henkemeyer *et al*., 1995; Lin *et al*., 1998; Lee *et al*., 1999), indicating that a delicate balance of Ras activity is essential for the survival of neurons. The potential role of synGAP in activity-dependent regulation of Ras at synapses could be important for regulating the action of growth factors and refinement of synaptic connections.

To enable identification of downstream pathways that are deregulated in the absence of synGAP, we generated mice with a targeted deletion, and with a conditional deletion in the synGAP gene. As also shown by other groups (Komiyama *et al*., 2002; Kim *et al*., 2003), we find that homozygous mutants with a deletion of synGAP (*ko*) die between postnatal days 1 and 2 (P1 and P2). Here we report that the brains of *ko* mutants on P0 and P1 contain significantly more neurons undergoing apoptosis, as measured by caspase-3 activation, than brains of *wt* animals. We also show that conditional *ko* mutants that begin to lose synGAP expression in forebrain pyramidal neurons between 1 and 2 weeks of age also have significantly higher activation of caspase-3 in those neurons than age-matched controls. The level of neuronal apoptosis and the survival of the mice depend on the extent of reduction of synGAP. Our results show that synGAP plays an important role in regulating or coordinating signal transduction pathways that trigger apoptosis.

Correspondence: Dr M. B. Kennedy, as above.
E-mail: kennedym@its.caltech.edu

**Present address*: Swiss Federal Institute of Technology, Laboratory of Behavioural Neurobiology, Schorenstrasse 16, 8603 Schwerzenbach, Switzerland.

†*Present address*: AmCyte Inc., 2825 Santa Monica Blvd., Suite 200, Santa Monica, CA 90404–2429, USA.

Received 8 September 2004, revised 10 November 2004, accepted 15 November 2004

doi:10.1111/j.1460-9568.2005.03908.x

Materials and methods

Generation of mice with a floxed allele of synGAP

A targeting construct containing exons 4–9 and three lox-P sites was constructed and introduced into embryonic stem (ES) cells as previously described (see Fig. 1; Vazquez *et al*., 2004). The ES cells were transfected with the Cre-expressing vector pOG231 (kindly provided by Dr Henry Lester at Caltech) by electroporation. Twenty-eight G418-sensitive clones were identified. Two of the clones had complete deletion of sequences between exons 4 and 9 of synGAP (knockout; *ko*) and the rest had loxP sites flanking the sequences between exons 4 and 9 (floxed; *flox*). One clone with the *flox* genotype that had a normal karyotype was used for injection into blastocysts to generate chimeras. Injections and breeding of chimeras were performed by the Transgenic Mouse Core Facility at Caltech. The synGAP *flox* mutation described here is maintained in a homozygous line and has been back-crossed onto a C57/B6 background. All animal procedures were approved by the California Instititute of Technology Animal Care and Use Committee.

Generation of mice with a conditional synGAP-ko mutation

Excision of the synGAP coding sequence was accomplished by crossing mice bearing the synGAP *flox* allele with a line of mice expressing a transgene encoding cre recombinase under control of the promoter for the α-subunit of CaMKII (αCaMKII). This promoter drives expression in excitatory forebrain neurons beginning about 1 week after birth (Schweizer *et al*., 2003). We obtained the most effective reduction of synGAP expression by creating a line of mice containing the transgene, one *flox* allele, and one *ko* allele of synGAP (αCaMKII:cre; synGAP*flox/–*). To obtain this line, we first bred the transgene (αCaMKII:cre) into a heterozygous synGAP *ko* background. The resulting αCamKII:cre; synGAP+/– mice were then crossed with the synGAP *flox* (synGAP*flox/flox* or synGAP*flox/+*) line to create conditional synGAP-*ko* mice (αCamKII:cre; synGAP*flox/–*), hereafter referred to as cond-*ko*'s. For our initial crosses, the αCaMKII:cre transgene was in a 129vJ background and the synGAP+/– strain had a mixed 129vJ/C57Bl6 background (the heterozygous *ko*'s breed poorly when fully outcrossed into C57Bl6). The synGAP*flox* gene was outcrossed into a C57Bl/6 background.

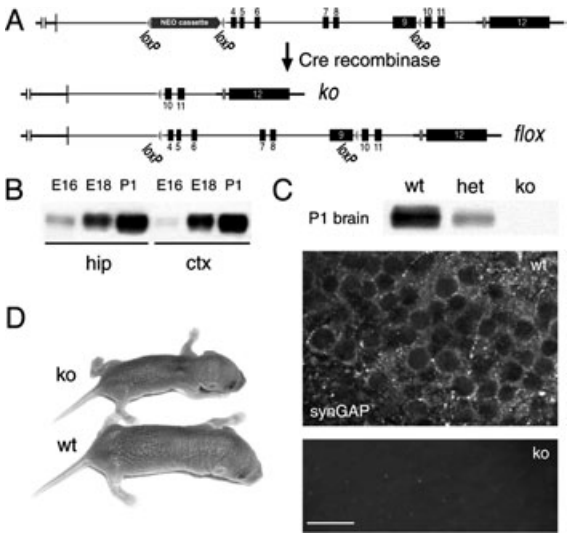

FIG. 1. Construction of a synGAP knockout mouse. (A) The targeting construct included a Neo cassette flanked by Lox P sites inserted into intron 3 of the synGAP gene, and an additional downstream Lox P site within intron 9. Expression of Cre recombinase in recombinant ES cells resulted in either deletion of exons 4–9 of the synGAP gene (*ko*) or removal of the Neo cassette, leaving two Lox P sites flanking exons 4–9 (*flox*). (B) Immunoblot comparing synGAP expression levels during hippocampal and cortical development in *wt*. (C) SynGAP is not expressed in *ko* brains. (top) Immunoblot confirming that all four isoforms of SynGAP protein are absent in brain extracts of *ko* mice and are reduced in heterozygous (*het*) mice at P1 compared with *wt.* (middle) Images from sagittal sections taken at P1 showing immunofluorescently labeled synGAP in hippocampal CA1 pyramidal neurons. (bottom) The punctate staining of synGAP in *wt* mice is completely absent in *ko* mice. (D) SynGAP *ko* mice are smaller in size than *wt* littermates on P1. They are weak, display impaired motor skills and trembling, and generally die by P2. Scale bar, 20 μm.

Genotyping

Genomic DNA was isolated from mouse tails. The following primers were used to determine the allele of the synGAP gene by PCR:
MGIN-11, 5′-GAGAGAGATGGAGGGTCACTTGAG-3′;
MGEX9-1, 5′-CGGATGCTATGTGCAGTGCTGGA-3′; and
Lox-DS, 5′-GAAGAGGAGTTTACGTCCAGCCAAGCT-3′.
PCR cycles started with denaturation of DNA at 94 °C for 2 min followed by 35 cycles of the following three conditions: 95 °C, 30 s; 58 °C, 30 s; and 72 °C, 2 min; followed by a final extension at 72 °C for 10 min. The PCR products were fractionated on 0.9% agarose gels. A fragment of 1.9 kb indicated the flox allele, 1.8 kb indicated the wt allele and 1.7 kb indicated the ko allele. PCR screens for the cre transgene were performed with two primers: Cre-up, 5′-CCAGCAA CATTTGGGCCAGC-3′; and Cre-low, 5′-CGGAAATCCAT CGCTC GACC-3′. PCR cycles started with denaturation of DNA at 95 °C for 2 min followed by 35 cycles of the following three conditions: 95 °C, 30 s; 58 °C, 30 s; and 72 °C, 2 min. The presence of the transgene was indicated by a 400-bp PCR product detected on a 2% agarose gel.

Measurement of synGAP by quantitative immunoblotting

We collected brains at embryonic day 16 (E16), E18, P0, P1 (*ko* line) or at 2 or 8 weeks of age (cond-*ko* line). Animals at P0 and P1 were anaesthetized by hypothermia, and older animals by exposure to an excess of CO_2. Animals were killed by decapitation and the brain rapidly removed. For experiments with cond-*ko* mice, the right hemisphere was frozen in powdered dry ice and stored at −80 °C until sectioned with a cryostat. Hippocampus and cortex were dissected from the left hemisphere and homogenized at 900 r.p.m. in Teflon-glass homogenizers in RIPA lysis buffer (50 mM Tris, pH 8, 2 mM EDTA, pH 8, 150 mM NaCl, 1% Nonidet P-40, 0.5% Deoxycholate, 0.1% SDS, 0.5 mM DTT) containing a cocktail of protease inhibitors (Complete™, Roche, Nutley, NJ, USA). Protein concentration was determined by the bicinchoninic acid (BCA) method (Pierce, Rockford, IL, USA) with bovine serum albumin as a standard. Aliquots of protein (10 μg) from cond-*ko*, mini and heterozygous control littermates were loaded in pairs, fractionated by SDS-PAGE and electrophoretically transferred to PVDF membranes (Bio-Rad Laboratories, Hercules, CA, USA). Membranes were blocked for 2 h in TBS, 0.1% Tween-20 (TBST), 5% non-fat milk at room temperature (RT) and incubated with rabbit anti-synGAP antibodies (Affinity BioReagents, Golden, CO, USA, 1 : 2000) in TBST, 1% NGS ON at 4 °C. They were washed three times for 10 min each in TBST, then incubated for 1 h at RT in secondary antibodies (Alexa488, Molecular Probes, Eugene, OR, USA, 1 : 200) diluted in TBST. After three washes in TBST and a rinse with distilled water, membranes were dried and scanned on a STORM™860 scanner (Molecular Dynamics

Inc., Sunnyvale, CA, USA) at 825 V. The optical density of the protein bands was measured with ImageQuant software (Molecular Dynamics). Two independent sets of gels with duplicate pairs were quantified per sample group.

Immunoblots of brains from synGAP heterozygotes and *ko*'s were performed similarly, except that protein was transferred to nitrocellulose membranes (Schleicher & Schuell, BioScience, Keene, NH, USA) and bands were visualized by chemiluminescence with SuperSignal® reagents from Pierce.

Histology and immunohistochemistry

Embryos at E18, and pups at P0 and P1 ($n = 2$–3 per genotype, from 2–3 different litters) were anesthetized by hypothermia and perfused through the ascending aorta with 4% paraformaldehyde and 15% saturated picric acid in 0.15 M phosphate buffer (pH 7.4). The fixation was preceded by a short rinse with phosphate-buffered saline (PBS; 10 mM $NaHPO_4$, 120 mM NaCl, pH 7.4). After postfixation for 48 h in the same fixative, brains were transferred to sodium citrate buffer (0.1 M citric acid mixed with 0.2 M Na_2HPO_4 to reach pH 4.5) and incubated overnight at RT (Fritschy *et al*., 1998). The tissue was then transferred into 80 mL fresh citrate buffer and irradiated in a microwave oven at medium power for 30 s to unmask protein antigens. After cooling for 15 min, the tissue was rinsed in PBS. Cryoprotection was achieved by immersion in 10% sucrose in PBS for 3 h, followed by 30% sucrose for 24 h. Sagittal sections (50 μm) were cut on a vibratome and stored in antifreeze solution (50 mM phosphate buffer, 15% glucose, 30% ethylene glycol) at −20 °C until further processing.

Every sixth section (300 μm apart) was Nissl-stained with cresyl violet to assess histological changes in synGAP *ko* brains. Changes in protein expression and localization were detected immunohistochemically using rabbit anti-synGAP (Affinity BioReagents, 1 : 500) and rabbit anti-cleaved caspase-3 (Cell Signaling Technology, Beverly, MA, USA, 1 : 100) antibodies. To evaluate the specificity of the cleaved caspase-3 antibody reactivity, control sections were incubated with antibody pre-absorbed with blocking peptide (Cell Signaling Technology). Additional controls included incubation with secondary antibodies alone.

Free-floating sections were washed in Tris-saline buffer, TBS (50 mM Tris, 150 mM NaCl, pH 7.4) and preblocked in TBS containing 0.25% Triton X-100 and 10% normal goat serum (NGS) for 30 min at room temperature. Sections were incubated overnight at 4 °C in primary antibody solution diluted in TBS, 0.25% Triton X-100, 4% NGS. Sections were then washed three times for 10 min each in TBS and incubated for 30 min at RT in secondary antibodies [goat anti-rabbit Alexa488 or goat anti-mouse Alexa568 (Molecular Probes, 1 : 500 each)] diluted into TBS, 4% NGS. Cell nuclei were visualized by incubating the slices in 0.25 mg/mL Hoechst 33342 (Molecular Probes) in TBS for 15 min at RT. Sections were washed again three times for 10 min in PBS, mounted on poly-L-lysine-coated slides (Electron Microscopy Science, Hatfield, PA, USA), air-dried and coverslipped with a drop of ProLong® anti-fade reagent (Molecular Probes).

Brain sections of the right hemisphere of synGAP cond-*ko*, mini and control mice were cut at 15 μm with a cryostat at −20 °C, mounted onto poly-L-lysine-coated slides (Electron Microscopy Science) and air-dried at RT for 30 s. One series of sections per brain was Nissl-stained with cresyl violet to assess histological changes in mutant brains. Sections used for immunohistochemistry were fixed in methanol at −20 °C for 10 min, transferred into PBS buffer and processed as described for free-floating sections.

Image acquisition and quantification

A Zeiss Axiovert 200 microscope was used for epifluorescence and light microscopy. Images were acquired with a Plan-NeoFluar 5×/0.15 or Plan-Apochromat 63×/1.4 oil objective and a high-resolution CCD camera (Axiocam MRm, Zeiss, Jena, Germany) under the control of a computer equipped with AxioVision 3.1 (Zeiss). Exposure times were set so that pixel brightness was never saturated, and were held constant during acquisition of all images (1300 × 1030 pixels) for each experiment. For high-magnification images of fluorescently labeled brain slices, 16 optical sections ('z-sections'; 300 nm intervals) were acquired and deconvolved with the 'Regularized Inverse Filter' method (AxioVision software). For visual display and figures, sections were summed and projected in the z-dimension (ImageJ software, NIH, Bethesda, MD, USA).

Quantitative analysis of sections stained for synGAP and activated caspase-3 were performed on low-magnification images of the hippocampus, neocortex and cerebellum. Brightness of fluorescence was measured in five fields (100 × 100 pixels each) per section in CA1 stratum radiatum or cortex layers I–V and averaged from six brain slices per animal ($n = 4$ per genotype) using KS300 software (Zeiss). Data were statistically compared using ANOVA and the Tukey–Kramer multiple comparison test, and significance was accepted as $P < 0.05$.

The brightness of the fluorescent staining of activated caspase-3 allowed us to count the labeled cells at low magnification in images (1300 × 1030 pixels) acquired with a 5× Plan-NeoFluar objective. For every animal ($n = 2$–3 synGAP *ko* and wild-type littermates; $n = 2$–4 mini's, normal cond-*ko*'s and heterozygous littermate controls) six images from six different brain slices were taken from the dorsal hippocampal formation, primary somatosensory cortex and cerebellum. The number of activated caspase-3-positive cells counted per section in each brain area was averaged and statistically compared between genotypes using an unpaired Student's *t*-test (synGAP *ko* and wild type) or ANOVA and the Tukey–Kramer Multiple Comparison test (synGAP cond-*ko* and heterozygous controls). Significance was accepted as $P < 0.05$. Both image acquisition and quantification were performed blind to the experimental condition.

Results

Construction of synGAP knockout and conditional knockout mice

We generated a synGAP knockout mouse line (Vazquez *et al*., 2004), and a conditional mutant line with a single targeting construct. The targeting construct contained three loxP sites (Fig. 1A) enclosing a neomycin selection cassette and genomic DNA including exons 4–9 of synGAP. After transfection and selection for homologous recombination, mutant ES cells were transfected again with a vector that transiently expresses Cre-recombinase (see Materials and methods), and screened for one of two mutations: complete deletion of exons 4–9 (*ko*), and introduction of loxP sites surrounding exons 4–9 (*flox*). One ES cell colony bearing the synGAP *flox* allele was used to generate a line of synGAP *flox* mice. To delete synGAP in forebrain principal neurons beginning at approximately 1 week old, we crossed mice bearing the synGAP *flox* allele with a line of transgenic mice expressing cre recombinase under control of the αCaMKII promoter (αCaMKII:cre, Schweizer *et al*., 2003). We found that expression of Cre in the synGAP*flox/flox* background never reduced the level of synGAP below that of heterozygous *ko*'s, presumably either because of a low rate of recombination and/or a low rate of turnover of synGAP protein. Therefore, we introduced the αCaMKII:cre transgene into the synGAP *ko* background to produce αCaMKII:cre; synGAP+/– offspring. We

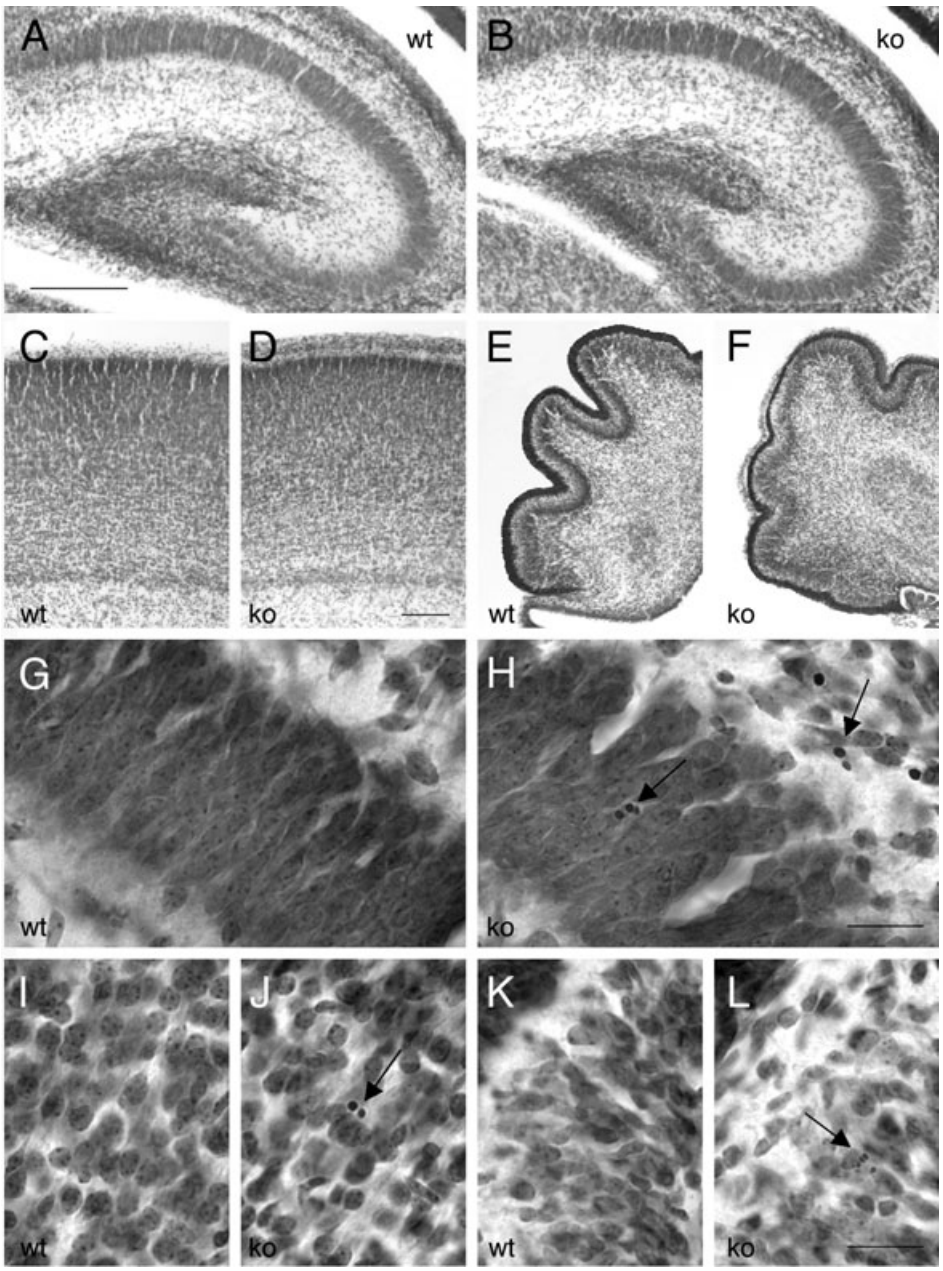

FIG. 2. Morphology of hippocampus, cortex and cerebellum at P1. (A–D) Nissl-stained sagittal sections of hippocampus (A and B) and cortex (C and D) of *wt* and *ko* mice. The cytoarchitecture of the hippocampus and cortex appears normal in *ko* mice. (E and F) The cerebellum is underdeveloped in *ko* mice with reduced folding of the lobes compared with *wt* litter mates. (G and H) Higher magnification images of Nissl-stained sections of hippocampal area CA1 reveal many more pyknotic nuclei in stratum pyramidale and stratum oriens (arrows) of *ko* mice than of *wt* controls. (I and J) Pyknotic nuclei are found in all neocortical layers of *ko* mice (e.g. arrow). (K and L) Less dense cell layers and pyknotic nuclei are found in the Purkinje cell layer and internal granule cell layer of cerebellar sections (arrow). Scale bars: A, 200 μm; D, 100 μm; H and L, 20 μm.

then crossed these offspring with synGAP*flox/flox* mice to produce progeny, approximately one-quarter of which had the compound heterozygous genotype, αCaMKII:cre; synGAP *flox/–*. Mice with this genotype exhibited progressive reduction of synGAP protein below levels present in synGAP heterozygotes beginning ∼1 week after birth. In this study, we compared synGAP *ko* mice with cond-*ko* mice.

Phenotype of synGAP ko mice

In wild-type brains, synGAP expression increases rapidly in the hippocampus and cortex between E16 and P1 (Fig. 1B). The synGAP protein comprises at least four major splice variants, all encoded by the same gene (Chen *et al*., 1998). Immunostaining reveals that it is located in puncta along neuronal somata and dendrites, most prominently in the CA fields of the hippocampus (Fig. 1C). It is expressed at similar levels in all neocortical layers, and in cerebellar Purkinje cells; and at lower levels in olfactory bulb, thalamus, striatum and brainstem (data not shown). Deletion of synGAP (*ko*) eliminated all splice variants and eliminated immunostaining in all brain regions at P1 (Fig. 1C). The *ko* pups appear normal at birth, but do not grow and by P1 become noticably smaller than their littermates (Fig. 1D). As previously reported, they die before the end of P2 (Vazquez *et al*., 2004).

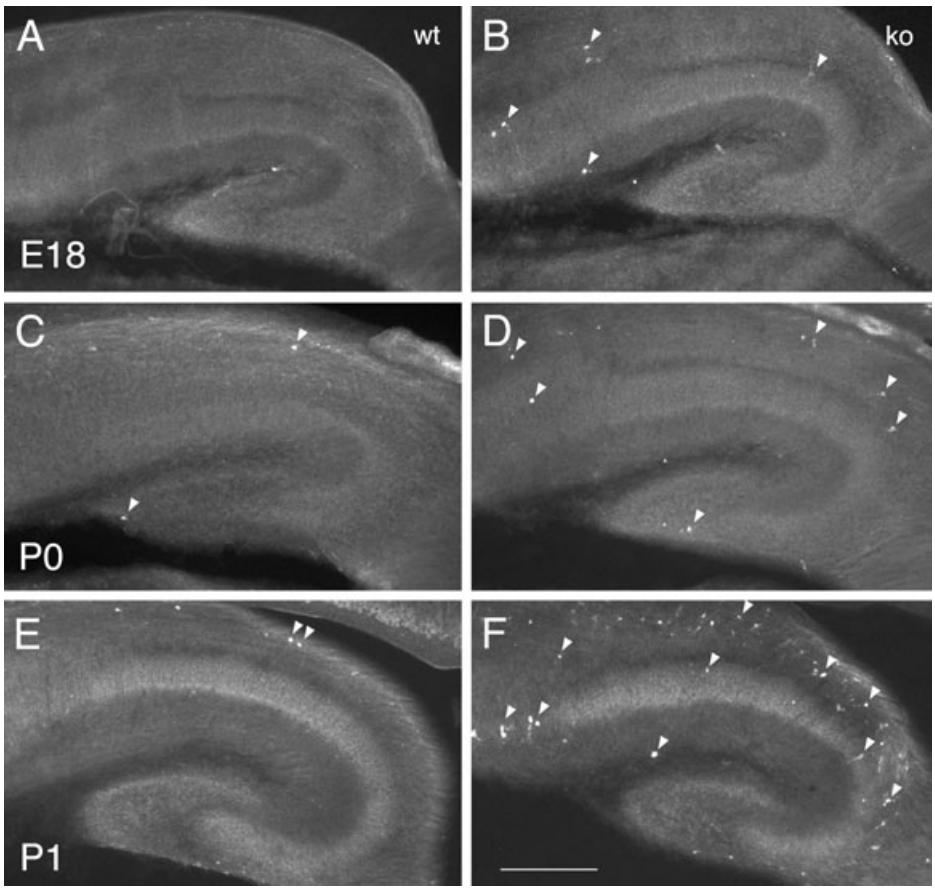

FIG. 3. Increased apoptosis in *ko* brain. Low-power images of brain sections at E18 (A and B), day of birth (P0; C and D) and P1 (E and F) of *wt* (A, C and E) and *ko* mice (B, D and F). Immunofluorescent staining with anti-activated caspase-3 antibodies of sections of the hippocampus showing higher numbers of activated caspase-3-positive cells per section (arrowheads indicate examples) in *ko* mice compared with *wt* littermate controls. Differences are more pronounced on P1 with highest numbers of activated caspase-3-positive cells in stratum oriens and stratum pyramidale. The data are quantified in Fig. 4. Scale bar, 200 μm.

Increased neuronal apoptosis in brains of synGAP ko mice

Nissl-stained sections of brains from *ko* and *wt* mice at P1 revealed no gross anatomical differences in hippocampus and cortex from the two genotypes (Fig. 2A–D). However, the cerebelli of mutant mice were underdeveloped in all three animals examined (Fig. 2E and F), suggesting a defect in cell signaling during early cerebellar development. Examination of *ko* brains at higher power revealed more pyknotic nuclei in the CA areas of the hippocampus, cortical layers I–VI and the cerebellar Purkinje cell layer than were present in these brain areas in *wt* mice of the same age (Fig. 2G–L, arrows).

To determine whether the pyknotic nuclei reflect an increase in apoptotic cell death, we stained sections with an antibody against activated caspase-3, a cysteine protease that is a key degradative enzyme in apoptosis (Rami, 2003). We found that many more neurons stain positively for activated caspase-3 in the brains of synGAP *ko* mice than in their wild-type littermates. The first significant differences in activated caspase-3 between the genotypes can be seen in the hippocampus at E18 and is also evident at P0 (Figs 3A–D and 4), a time at which the *ko* pups are superficially indistinguishable from *wt*. Thus, the increased apoptosis is not simply a result of extreme poor health of the mutants. By P1, a significant difference in the number of activated caspase-3-positive neurons between *ko* and *wt* mice is also evident in the cerebellum and cortex (Figs 3E and F, and 4).

Higher power images revealed that the activated caspase-3-positive cells have the morphology of neuronal somas (Fig. 5A and B). In the hippocampus, most of these apoptotic neurons are found in stratum oriens and the pyramidal layer, whereas stratum radiatum, dentate gyrus and hilus are nearly devoid of activated caspase-3-positive cells. Apoptotic neurons were distributed throughout cortical layers I–VI and the Purkinje cell layer of the cerebellum (Fig. 5C and D).

An increase in levels of activated caspase-3 is also visible on immunoblots of homogenates of brains of homozygous *ko*'s, as compared with brains from *wt* and *het* mice at P1 (Fig. 5E). We hypothesize that the presence of abnormally high numbers of neurons undergoing apoptotic death may account, entirely or in part, for the observed weakening and eventual death of the homozygous synGAP *ko* mutants.

*Phenotype of synGAP cond-*ko *mice*

Mice heterozygous for synGAP have approximately half as much synGAP in their brains as *wt*, both at P1 and as adults, but they do not show elevated levels of neuronal apoptosis (data not shown). We investigated whether reduction of synGAP below the level present in heterozygote brains would increase the number of apoptotic neurons in a conditional synGAP *ko* in which the loss occurs at a stage of development well beyond P1. To generate such a conditional-*ko*, we introduced a transgene expressing cre-recombinase driven by the αCaMKII promoter into a synGAP*flox/–* background, as described in the Materials and methods. The spatial and temporal pattern of

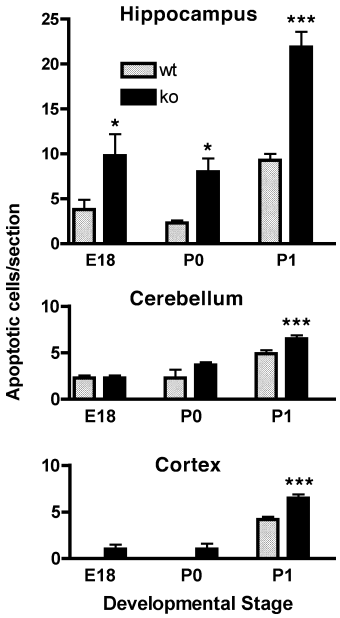

FIG. 4. Apoptotic cells/section (mean ± SEM), visualized by staining with anti-activated caspase-3 (see Fig. 3), in sections of hippocampus, cerebellum and cortex from *wt* and synGAP *ko* mice at E18, P0 and P1. Activated caspase-3-positive cells were counted in individual optical fields as described in the Materials and methods, and averaged from 4–6 brain sections per animal. Sections from hippocampus, cortical layers I–VI and cerebellum were counted from two animals at E18 and P0 and three animals at P1 for each genotype. $*P < 0.05$, $***P < 0.001$ (unpaired Student's *t*-test).

Cre/loxP recombination induced by the αCaMKII:cre transgene line that we used has been described recently by Schweizer *et al*. (2003). Cre-induced recombination of an alkaline phosphatase gene in a reporter mouse was first detectable by staining in the hippocampus at P17 and then gradually increased to adult levels by P34. Recombination was restricted to principal neurons of the forebrain with highest levels in CA1, dentate gyrus and cerebral cortex (Schweizer *et al*., 2003).

Mice from seven litters, three from crosses of αCaMKII:cre; synGAP+/– with αCaMKII:cre; synGAP*flox*/+ and four from crosses of αCaMKII:cre; synGAP+/– with synGAP*flox*/+, were individually marked with ink using a micro-tatoo applicator and their weight was recorded every second day from 5 to 28 days after birth. We followed 17 pups with the genotype αCaMKII:cre: synGAP*flox*/– (cond-*ko*) and 19 littermate controls with genotype synGAP*flox*/– or α-CaMKII:cre: synGAP+/–. Thirteen of the cond-*ko* mice were phenotypically normal up to the fourth postnatal week and their weight was statistically indistinguishable from heterozygous littermate controls. However, four of the cond-*ko* animals were significantly smaller at P7. By 2 weeks after birth, their health started to decline. Signs of distress included lack of locomotion and weight loss. We refer to this subset of cond-*ko* mice as 'mini's' and the rest as 'normal cond-*ko*'s'. All of the mini's died by 3 weeks after birth (Fig. 6). Although the normal cond-*ko* mice remained generally healthy, four of the 13 had reduced weight gain after 3 weeks, reflected in the large error bars at day 24 in Fig. 6. In addition, many of the normal cond-*ko* mice became hyperactive (sometimes running in circles from the top to the bottom of their cage) when attempts were made to handle them or their cages.

Levels of synGAP protein correlate with severity of the cond-ko phenotype

Of 103 cond-*ko*'s produced in the colony, 13 (12.6%) have had the mini phenotype. To determine whether the two distinct cond-*ko* phenotypes are caused by differences in the level of conditional deletion of synGAP, we used semi-quantitative immunoblots to monitor levels of synGAP protein in progeny of various genotypes.

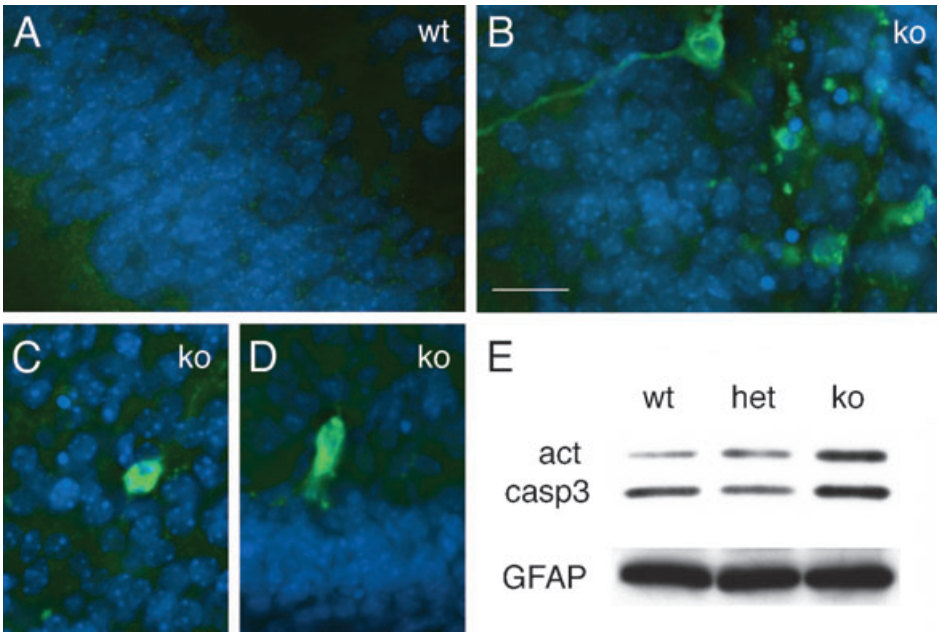

FIG. 5. Increased neuronal cell death in brain of *ko* mouse on P1. (A and B) Higher magnification pictures of area CA1 in *wt* (left) and *ko* (right) brain double-stained for cell nuclei (Hoechst 33342, blue) and activated caspase-3 (green). Note the neuronal appearance of activated caspase-3-positive cells and the presence of condensed nuclei in the *ko* hippocampus. (C) Double-staining of nuclei and activated caspase-3 (green) in the neocortex of a *ko* mice. (D) Double-staining of nuclei and activated caspase-3 (green) in the Purkinje cell layer of the cerebellum of a *ko* mouse. (E) Immunoblot of hippocampal extracts of *wt*, *het* and *ko* littermates on P1 with antibody against activated caspase-3 and GFAP. Whereas levels of activated caspase-3 are significantly increased in *ko* mice compared with *wt* and *het* mice, GFAP levels remain unchanged in all genotypes. Scale bar, 20 μm.

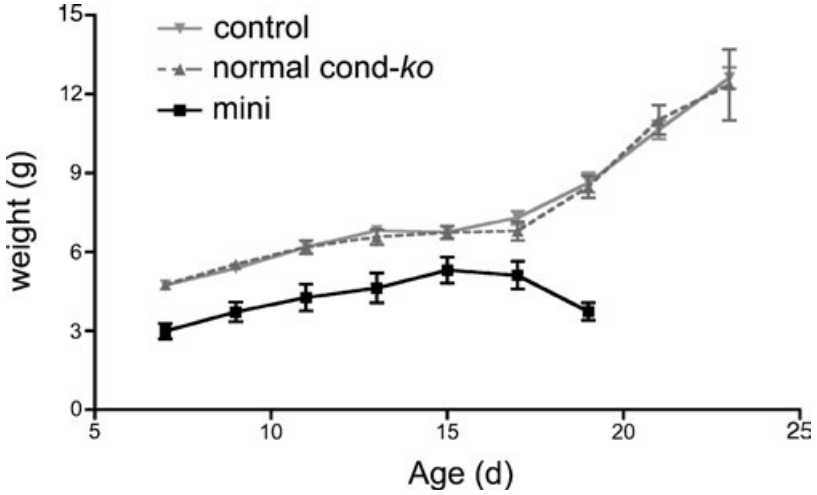

FIG. 6. Two distinct phenotypes of synGAP conditional mutant mice. Weights of individually marked pups were recorded from seven different litters (mean ± SEM). A total of 19 controls and 17 cond-*ko*'s were monitored during the first four postnatal weeks. Within the group of cond-*ko*'s, four (■) were significantly smaller, started to weaken around day 14 and died before 3 weeks of age. We refer to these as 'mini's'. The weight of the remaining 13 cond-*ko*'s, which we refer to as normal cond-*ko*'s, was indistinguishable from heterozygous littermate controls. However, after day 21, four of the normal cond-*ko*'s had significantly lower weights than their littermate controls, as reflected in the large error bars at day 24.

We first performed a series of control quantitative immunoblots on homogenates of hippocampus and cortex from 8-week-old mice to compare levels of expression of synGAP protein among the following six genotypes ($n = 2$ of each); *wt* [synGAP+/+], *wt* plus transgene [αCaMKII:cre; synGAP+/+], synGAP heterozygote [synGAP+/–], homozygous *flox*ed synGAP [synGAP*flox/flox*], heterozygous *flox*ed synGAP [synGAP*flox/–*] and heterozygous *flox*ed synGAP plus transgene [αCaMKII:cre; synGAP*flox/+*]. We found that neither cre expression alone nor the presence of two *loxP* sites in the synGAP gene affects levels of expression of synGAP protein. We also found no statistical difference in expression of synGAP between synGAP+/– and synGAP*flox/–* mice (all $P > 0.05$, ANOVA). Based on these findings, mice of genotypes synGAP*flox/–* or αCamKII:cre; synGAP+/– were used interchangeably as controls in the following experiments.

We then compared levels of synGAP at 2 weeks after birth in hippocampus and cortex of three mini's, six normal cond-*ko*'s and 12 heterozygous littermate controls. In both brain regions, the level of synGAP in mini's was reduced to 40–50% of heterozygotes, and in normal cond-*ko*'s it was reduced to 75% of heterozygotes (Fig. 7A and B). These levels correspond to 20–25% of *wt* in mini's and 37.5% of *wt* in normal cond-*ko*'s. SynGAP immunoreactivity in fixed brains of normal cond-*ko*'s and mini's was significantly reduced in the dendritic fields compared with their heterozygous littermates (Fig. 7C). There were no apparent regional differences in reduction of synGAP between mini's and normal cond-ko's. We did not observe mosaic staining patterns in brains from either genotype. Measurements of the brightness of fluorescent labeling in CA fields and dentate gyrus (data not shown) revealed the same extent of reduction of synGAP levels in each genotype that we obtained from analysis of immunoblots. We conclude that 75% loss of synGAP constitutes a threshold below which growth is impaired and the animal eventually dies.

Levels of synGAP protein correlate with severity of neuronal apoptosis

To determine whether loss of synGAP can influence neuronal apoptosis when it takes place between 1 and 3 weeks after birth, we counted cells containing activated caspase-3 in brains from synGAP cond-*ko* mice. Alternating sections from brains of two mini's, two normal cond-*ko*'s and two heterozygote littermate controls fixed at 2 weeks after birth were stained with Nissl stain or immunohistochemically with anti-activated caspase-3 antibodies. The sections were taken from one hemisphere of the same brains that were homogenized for the immunoblot analysis described in Fig. 7 (see Methods).

As with *ko* mice, we found no gross anatomical differences among the brains of the three groups; however, we found significantly more activated caspase-3-positive neurons per brain section in several brain areas of mini's and normal cond-*ko*'s compared with control heterozygous littermates (Fig. 8, Table 1). As expected from the expression pattern of cre recombinase conferred by the αCaMKII promoter, we found more activation of caspase-3 in the cell body layers of the hippocampus (CA stratum pyramidale and DG stratum granulare), but not in stratum oriens or stratum radiatum. Although some of the interneurons present in oriens and radiatum express synGAP (Zhang *et al*., 1999), none of them expresses CaMKII (Liu & Jones, 1996), and thus they would not be expected to express cre recombinase. This pattern of activated caspase-3 contrasts with the pattern we observed in brains from *ko* animals, which included an increase in active caspase-positive neuronal cell bodies in stratum oriens, as well as in pyramidale (Fig. 3). In the cerebral cortex, we found significantly more neurons containing activated caspase-3 in layers II–VI and in the ventricular zone in mini's compared with heterozygotes, but not in layer I, which lacks positive staining for αCaMKII (Liu & Jones, 1996) (Fig. 8C and D; Table 1).

In two areas, stratum granulare of the dentate gyrus and layers II–VI of the cortex, mini's have many more neurons containing activated caspase-3 than do normal cond-*ko*'s. Because the mini's also have significantly greater reduction of synGAP expression than cond-*ko*'s, this finding means that the level of induction of apoptosis correlates with the level of reduction of synGAP.

These data show that neuronal apoptosis is increased in conditional synGAP-*ko* mutants at 2 weeks after birth, when the level of synGAP protein has begun to fall. The increase in apoptosis occurs only in pyramidal neurons in the forebrain, in which synGAP protein has been reduced due to expression of cre recombinase, and the increase is proportional to the loss of synGAP.

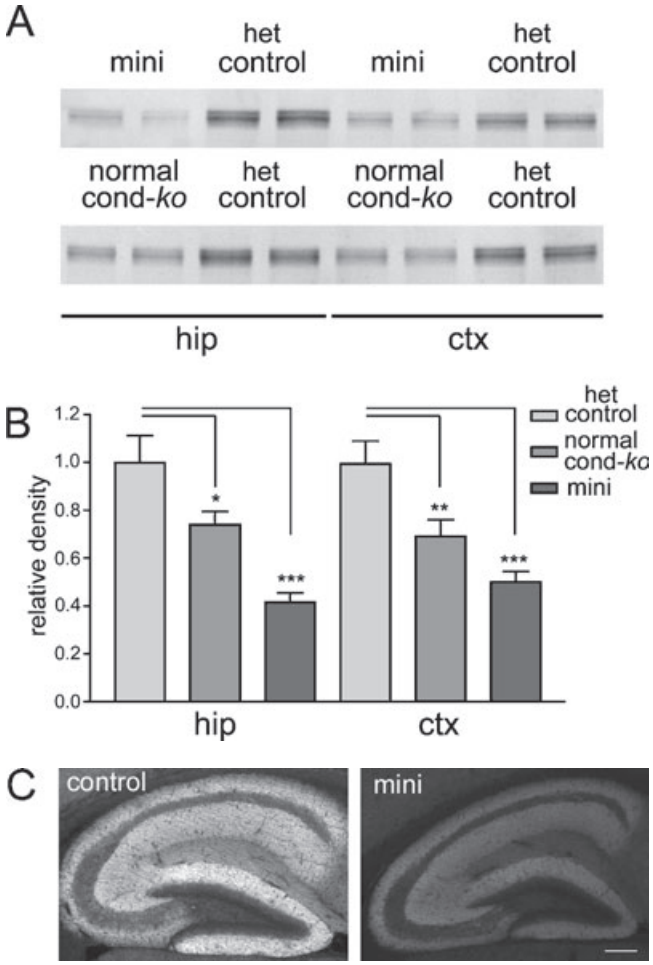

FIG. 7. Levels of synGAP protein in brains of synGAP cond-*ko*'s and heterozygous controls at 2 weeks after birth. (A) Representative immunoblots with anti-synGAP antibody of hippocampal and cortical extracts of mini's, normal cond-*ko* and control mice. Protein samples were run as duplicates. (B) Quantitative analysis of immunoblots was carried out as described in the Materials and methods. Densities of immunoreactive bands from cond-*ko*'s ($n = 6$) and mini's ($n = 3$) were normalized to values for heterozygous controls ($n = 12$). $*P < 0.05$, $**P < 0.01$, $***P < 0.001$. (C) Representative images of immunofluorescent staining with anti-synGAP antibody of hippocampal slices from 2-week-old heterozygous controls and mini's. Levels of synGAP protein in dendritic fields of hippocampi of mini's is greatly reduced compared with heterozygous control littermates. Scale bar, 100 μm.

*Increased apoptosis in 8-week-old cond-*ko *mice*

To determine whether the increased apoptosis in brains of cond-*ko* mice was restricted to the first few weeks after birth, we measured levels of synGAP and counted neurons containing activated caspase-3 in four normal cond-*ko* and four control heterozygote brains from 8-week-old mice. Nissl-stained sections revealed no histological differences. The reduction of synGAP protein in hippocampi from 8-week-old cond-*ko*'s was similar to that from 2-week-old cond-*ko*'s, but the reduction in the cortex was not as large (compare Figs 7A and B, and 9A and B). Thus, cre-mediated destruction of the synGAP gene did not increase between 2 and 8 weeks after birth. Caspase-3 activation was significantly increased compared with heterozygous controls in CA stratum pyramidale and DG stratum granulare of the hippocampus, but it was not increased in stratum oriens or radiatum (Table 2). In the cortex there was a significant increase in neurons with activated caspase-3 in layers II–VI in 8-week-old cond-*ko* mice compared with controls, but no significant difference in layer I or the ventricular zone (Table 2). The number of layer II–VI neurons containing activated caspase-3 was similar in 2- and 8-week-old cond-*ko* mice; however, the number of positive neurons in heterozygous controls was significantly lower at 8 weeks. As a result, the difference between cond-*ko* and control is statistically significant in the 8-week-old mice, but not in the 2-week-old mice (compare Tables 1 and 2). The difference between the controls may reflect decreased normal activation of caspase-3 in neurons of adult mice compared with those of 2-week-old mice. In summary, levels of synGAP and numbers of neurons with activated caspase-3 were similar in 2- and 8-week-old cond-*ko* mice and showed similar changes in comparison with heterozygous controls (Tables 1 and 2), consistent with a correlation between the level of synGAP protein and induction of apoptosis.

These data show that the level of neuronal apoptosis, as indicated by activation of caspase-3, is elevated in 8-week-old cond-*ko* mice compared with heterozygous controls. As also observed in 2-week-old cond-*ko* mice, the elevation of activated caspase-3 occurs only in neurons that are expected to express cre recombinase driven by the αCaMKII promoter, and thus to exhibit conditional knockout of the synGAP gene.

Discussion

In this study, we have shown that loss of synGAP, a synaptic Ras/Rap GAP protein, causes an abnormally high level of neuronal apoptosis, as indicated by the number of neuronal somas containing activated caspase-3. Caspase-3 is an effector caspase that is cleaved and activated by initiator caspases (Budihardjo *et al*., 1999; Shi, 2002). Its activation commits the cell to apoptosis. The first indication that loss of synGAP increases activation of caspase-3 came from our finding that mouse embryos and newborns with a homozygous knockout of synGAP have increased numbers of neurons in the hippocampus that are stained strongly with antibody against activated caspase-3. It is unlikely that the increased activation of caspase-3 in *ko*'s at this stage is caused by ill health because *wt* and *ko* littermates have no obvious differences in size or behavior at birth and both begin to feed normally. By P1, increased activation of caspase-3 becomes visible in neurons in the cerebellum and cortex of *ko* pups, as well as in the hippocampus. At this time, the *ko* pups stop growing, begin to weaken and usually die by the end of the day. It is possible that abnormal neuronal apoptosis in the brain contributes to their progressive weakening and death.

To better establish that deletion of synGAP is a direct cause of the increased activation of caspase-3, we generated conditional synGAP-*ko* mice that have synGAP at birth, but begin to lose the synGAP gene a few weeks after birth. This cond-*ko* line carries one copy of the synGAP deletion, one copy of a floxed synGAP gene and a transgene under control of the αCaMKII promoter that begins to drive expression of cre recombinase at 1 week after birth. When we examined the cond-*ko* mice at 2 and at 8 weeks old, we found that they indeed have an abnormally high number of neurons staining for activated caspase-3 compared with their *wt* or heterozygous littermate controls. Furthermore, a greater reduction in synGAP protein correlated with a larger increase in the number of neurons containing activated caspase-3. The level of reduction of synGAP in individual cond-*ko*'s varied considerably. We suspect that this may have resulted from variation in the efficiency of the action of the cre recombinase on the widely spaced loxP sites in the floxed synGAP gene. However, we did not observe mosaicism in the loss of synGAP in any of the mice. Mice with the most profound loss of synGAP protein (reduced to 20–

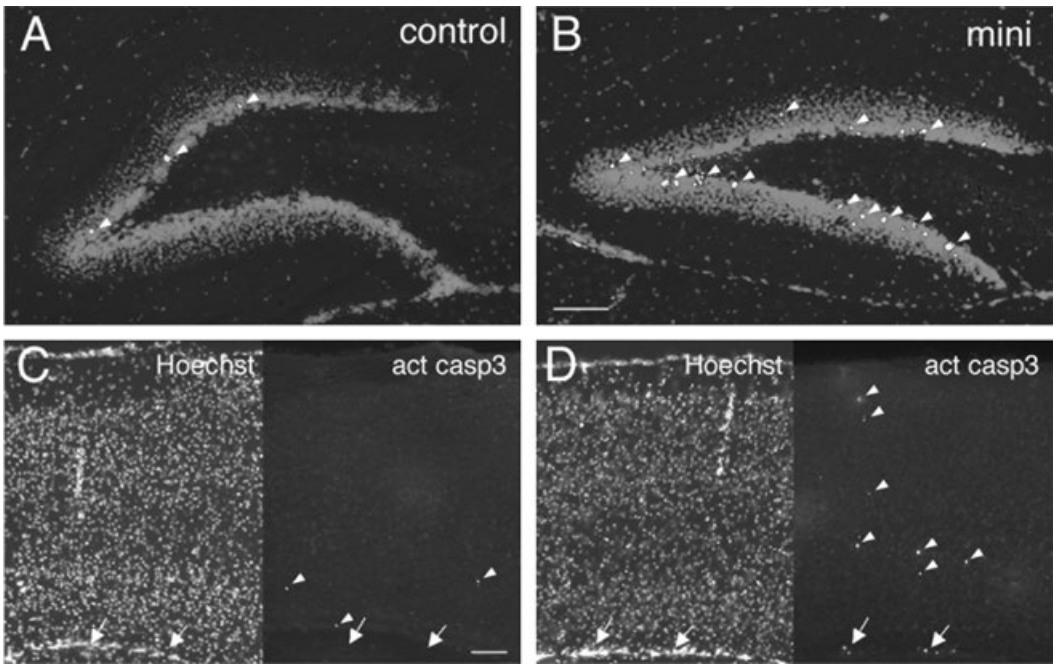

FIG. 8. Increased apoptosis in 2-week-old synGAP mini's. (A and B) Sections of the dentate gyrus of a 2-week-old heterozygous control (left) and a mini (right) double-stained for cell nuclei (Hoechst 33342) and activated caspase-3. Arrowheads indicate examples of activated caspase-3-positive cells; note the increase in such cells in the inner third of the granule cell layer in the dentate gyrus of the mini. (C and D) Immunofluorescent staining of 2-week-old cortical brain slices from a heterozygous control (C) and a mini (D). The two channels (left, Hoechst; right, activated caspase-3) are shown separately. A significant increase in apoptotic neurons is evident in cortical layers II–VI and in the ventricular zone (arrows) in brains of mini's compared with heterozygous littermate controls. Quantitative results are shown in Table 1. Scale bars, 100 μm.

TABLE 1. Activated caspase-3-positive cells in sections of brain from heterozygous controls, normal cond-*ko*'s and mini's at 2 weeks after birth

	Control	Normal cond-*ko*	Mini	Normal cond-*ko* vs. Control	Mini vs. Control	Mini vs. Normal cond-*ko*
CA						
Stratum oriens	1.0 ± 0.2	1.2 ± 0.3	0.9 ± 0.3	n.s.	n.s.	n.s.
Stratum pyramidale	0.4 ± 0.1	1.3 ± 0.4	1.5 ± 0.3	$P < 0.01$	$P < 0.001$	n.s.
Stratum radiatum	2.4 ± 0.4	2.3 ± 0.4	2.5 ± 0.5	n.s.	n.s.	n.s.
Dentate gyrus						
Stratum granulare	1.4 ± 0.3	3.8 ± 0.6	12.1 ± 2.0	$P < 0.001$	$P < 0.001$	$P < 0.001$
Cortex						
Layer I	0.8 ± 0.2	0.6 ± 0.2	1.1 ± 0.2	n.s.	n.s.	n.s.
Layers II-VI	2.3 ± 0.3	2.8 ± 0.4	6.9 ± 1.0	n.s.	$P < 0.001$	$P < 0.001$
Ventricular zone	1.5 ± 0.2	2.1 ± 0.3	2.6 ± 0.5	n.s.	$P < 0.05$	n.s.

Counts of activated caspase-3-positive cells in hippocampus and cortex from six sections per animal were averaged (number/section ± SEM; $n = 4$ for heterozygous controls, $n = 3$ for normal cond-*ko*'s, $n = 2$ for mini's). *P*-values were determined with unpaired one-tailed Student's *t*-test. n.s. = not significant.

25% of wild-type levels) were reduced in size, died within 2–3 weeks after birth and showed the highest number of neurons with activated caspase-3. These 'mini' mice were a minority (12.5%) among the cond-*ko*'s, most of which had a less profound reduction of synGAP protein levels (reduced to ~40% of *wt*). Cond-*ko*'s with the less severe reduction of synGAP grew normally for at least 8 weeks but, nevertheless, had significantly more neurons with activated caspase-3 in their brains than *wt*.

The location of the neurons containing activated caspase-3 supports the hypothesis that deletion of synGAP acts in a cell autonomous manner. In the *ko* pups, the highest numbers of activated caspase-3-positive neurons were found in stratum oriens and pyramidale of area CA, the cerebral cortex and the Purkinje cell layer of the cerebellum. Large numbers of cells with activated caspase-3 appeared very early in stratum oriens and had the morphology of interneurons. These likely represent GABAergic pioneer cells, some of which have been shown to undergo programmed cell death during the first postnatal weeks in *wt* mice, whereas others relocate within the hippocampal laminae and differentiate into the interneurons of adulthood (Jiang *et al*., 2001). SynGAP is expressed in a population of hippocampal interneurons cultured from E18 embryos (Zhang *et al*., 1999). Thus, it is possible that loss of synGAP from these neurons leads to exaggerated programmed death. Apoptotic neurons that appear in stratum pyramidale and in the cerebral cortex have the morphology of excitatory pyramidal neurons. These neurons and Purkinje cells in the cerebellum also express synGAP (data not shown). In the cond-*ko*, expression of cre recombinase is restricted to excitatory principal neurons in the forebrain by the αCaMKII promoter, leaving expression of synGAP in

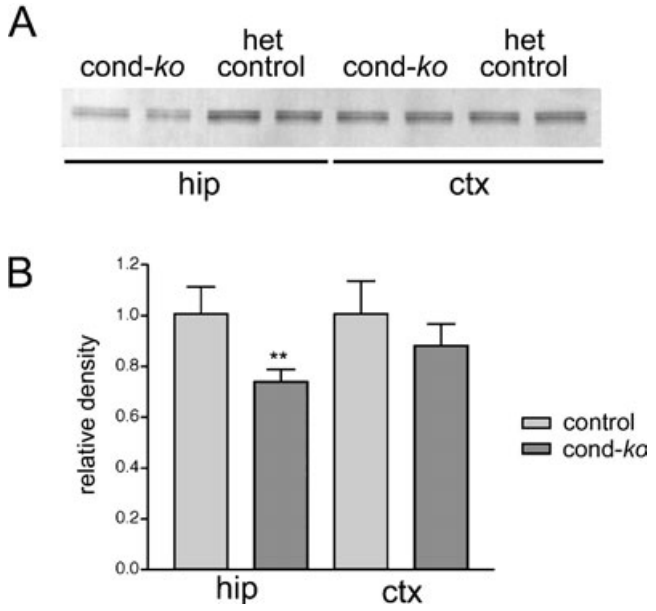

FIG. 9. Reduced levels of synGAP protein in 8-week-old synGAP cond-*ko* mice. (A) Representative immunoblot of hippocampal and cortical extracts from heterozygous controls and cond-*ko*'s with anti-synGAP antibody. Protein samples were run as duplicates. (B) Quantitative analysis of immunoblots reveals a statistically significant difference in levels of synGAP protein in hippocampus but not in cortex of 8-week-old normal cond-*ko* mice compared with heterozygous control littermates. Densities of bands in normal cond-*ko* samples ($n = 4$) were normalized to those of heterozygous controls ($n = 4$). $^{**}P < 0.01$.

TABLE 2. Activated caspase-3-positive cells in sections of brain from heterozygous controls and normal cond-*ko*'s at 8 weeks after birth

	Control	Normal cond-*ko*
CA		
stratum oriens	0.4 ± 0.2	0.7 ± 0.2
stratum pyramidale	0.3 ± 0.1	1.3 ± 0.3**
stratum radiatum	1.2 ± 0.2	1.4 ± 0.3
Dentate gyrus		
stratum granulare	2.3 ± 0.6	3.6 ± 0.5*
Cortex		
LI	0.3 ± 0.1	0.1 ± 0.1
LII–VI	1.3 ± 0.3	2.4 ± 0.5*
ventricular zone	0.8 ± 0.3	0.7 ± 0.3

Counts of activated caspase-3-positive cells in hippocampus and cortex from six sections per animal were averaged (number/section; mean ± SEM; $n = 4$ for heterozygous controls and for normal cond-*ko*'s). $^{*}P < 0.05$, $^{**}P < 0.01$ (unpaired Student's *t*-test).

interneurons intact. Correspondingly, we found increased activation of caspase-3 only among principal neurons in forebrain regions including stratum pyramidale, cortical layers II–VI and the dentate gyrus. We detected no differences in activated caspase-3 in neurons in CA stratum oriens, radiatum or cortical layer I, which contain mostly interneurons. Thus, increased numbers of apoptotic neurons are confined to neuronal classes in which the amount of synGAP is reduced.

The effect of loss of synGAP on activation of caspase-3 is somewhat surprising because in adult neurons synGAP is highly concentrated at synaptic sites. However, in developing neurons synGAP is distributed throughout the neuron; and even in adults a small portion appears localized to non-synaptic punctate structures that may be transport vesicles in the soma and dendritic shafts. Thus, synGAP may help to suppress triggering of apoptosis either through its actions at synapses, which then cascade into the soma, or via the action of a small portion of synGAP at extra-synaptic sites, or both. The possibility that synaptic synGAP may influence apoptotic pathways could be clinically important because Alzheimer's disease, which in its later stages causes severe neuronal death, has early symptoms that can be traced to synaptic dysfunction (Selkoe, 2002).

There are many possible mechanisms by which synGAP could influence activation of caspases and the onset of neuronal apoptosis. The most direct hypothesis is that loss of synGAP leads to an increase in basal activation of Ras, triggering apoptotic pathways. This general hypothesis is supported by the observations of Henkemeyer *et al*. (1995) on mice with a targeted deletion of p120-RasGAP, a ubiquitous Ras GTPase-activating protein. Their observations are similar to our findings. The p120-RasGAP *ko* mice die at E10.5 apparently because their vascular systems do not form properly. However, Henkemeyer *et al*. found extensive apoptotic cell death at E9 and E10 in the branchial arch and several brain regions including the telencephalon. Other tissues appeared relatively free of abnormal cell death. Thus, absence of p120-RasGAP, which is expressed embryonically, causes abnormal neuronal death as early as E9. These findings suggest that neuronal apoptotic mechanisms may be especially sensitive to the level of activated Ras. In contrast to p120-RasGAP, synGAP expression is restricted to the nervous system and begins around E14 to E16 (Fig. 1D), later than that of p120-RasGAP. This may explain why abnormal neuronal apoptosis appears later in synGAP *ko*'s than in the p120-RasGAP *ko*'s.

SynGAP and p120-RasGAP might regulate neuronal apoptotic pathways that are controlled directly by Ras. R-Ras, H-Ras and oncogenic Ras have been shown to promote apoptosis in cultured cells under particular conditions (Tanaka *et al*., 1994; Wang *et al*., 1995; Serrano *et al*., 1997). Another possibility is that synGAP, like p120-RasGAP, may be a precursor for an anti-apoptotic fragment that is generated by caspase-induced cleavage (Yang & Widmann, 2001, 2002). Yang and Widmann's data show that in situations where caspases are activated at low levels, p120-RasGAP is cleaved into an N- and C-terminal fragment generating a Ras-dependent anti-apoptotic response that prevents the cells from entering apoptosis. Thus, when p120-RasGAP is deleted, developing neurons may progress to full apoptosis more often. It remains to be determined, however, whether synGAP is also proteolytically cleaved by caspases to generate an anti-apoptotic fragment.

Several more complex possibilities are suggested by the recent results of Krapivinsky *et al*. (2004) published while this manuscript was being prepared. They show that, unlike p120-RasGAP, synGAP has a potent GAP action on Rap1, a distant member of the Ras family (Stork, 2003), as well as on Ras itself. Rap1 has a variety of actions on its effectors, depending on its cellular context (Stork, 2003). Its effectors can include p38, phosphatidylinositol-3 kinase, Raf-1, B-Raf and phospholipase-Cϵ. Rap-1 often acts antagonistically to the actions of Ras, and thus the precise mechanistic consequences of loss of synGAP in neurons are difficult to predict and will be the subject of considerable future investigation.

Acknowledgements

We thank Shannon O'Dell and Alan Rosenstein for expert technical assistance. We also thank members of the Kennedy laboratory for many helpful discussions. This work was supported by NIH grants NS17660 and NS28710 to M.B.K., and Swiss National Foundation fellowship 823A-064694 to I.K.

Abbreviations

αCaMKII:cre, cre recombinase transgene controlled by the alpha CaMKII promoter; CaMKII, Ca^{2+}/calmodulin-dependent kinase II; cond-ko, conditional synGAP knockout; ES cells, embryonic stem cells; flox, flanked by loxP sites; GAP, GTPase activating protein; ko, synGAP knockout; NMDA, *N*-methyl-D-aspartate; wt, wild type.

References

Bonni, A., Brunet, A., West, A.E., Datta, S.R., Takasu, M.A. & Greenberg, M.E. (1999) Cell survival promoted by the Ras-MAPK signaling pathway by transcription-dependent and -independent mechanisms. *Science*, **286**, 1358–1362.

Botella, J.A., Kretzschmar, D., Kiermayer, C., Feldmann, P., Hughes, D.A. & Schneuwly, S. (2003) Deregulation of the Egfr/Ras signaling pathway induces age-related brain degeneration in the *Drosophila* mutant vap. *Mol. Biol. Cell*, **14**, 241–250.

Budihardjo, I., Oliver, H., Lutter, M., Luo, X. & Wang, X. (1999) Biochemical pathways of caspase activation during apoptosis. *Annu. Rev. Cell Dev. Biol.*, **15**, 269–290.

Chen, H.-J., Rojas-Soto, M., Oguni, A. & Kennedy, M.B. (1998) A synaptic Ras-GTPase activating protein (p135 SynGAP) inhibited by CaM Kinase II. *Neuron*, **20**, 895–904.

Fritschy, J.M., Weinmann, O., Wenzel, A. & Benke, D. (1998) Synapse-specific localization of NMDA and GABA(A) receptor subunits revealed by antigen-retrieval immunohistochemistry. *J. Comp. Neurol.*, **390**, 194–210.

Henkemeyer, M., Rossi, D.J., Holmyard, D.P., Puri, M.C., Mbamalu, G., Harpal, K., Shih, T.S., Jacks, T. & Pawson, T. (1995) Vascular system defects and neuronal apoptosis in mice lacking ras GTPase-activating protein. *Nature*, **377**, 695–701.

Jiang, M., Oliva, A.A.J., Lam, T. & Swann, J.W. (2001) GABAergic neurons that pioneer hippocampal area CA1 of the mouse: morphologic features and multiple fates. *J. Comp. Neurol.*, **439**, 176–192.

Kennedy, M.B. (1997) The postsynaptic density at glutamatergic synapses. *Trends Neurosci.*, **20**, 264–268.

Kennedy, M.B. (2000) Signal-processing machines at the postsynaptic density. *Science*, **290**, 750–754.

Kim, J.H., Lee, H.K., Takamiya, K. & Huganir, R.L. (2003) The role of synaptic GTPase-activating protein in neuronal development and synaptic plasticity. *J. Neurosci.*, **23**, 1119–1124.

Kim, J.H., Liao, D., Lau, L.-F. & Huganir, R.L. (1998) SynGAP: a synaptic RasGAP that associates with the PSD-95/SAP90 protein family. *Neuron*, **20**, 683–691.

Komiyama, N.H., Watabe, A.M., Carlisle, H.J., Porter, K., Charlesworth, P., Monti, J., Strathdee, D.J., O'Carroll, C.M., Martin, S.J., Morris, R.G., O'Dell, T.J. & Grant, S.G. (2002) SynGAP regulates ERK/MAPK signaling, synaptic plasticity, and learning in the complex with postsynaptic density 95 and NMDA receptor. *J. Neurosci.*, **22**, 9721–9732.

Krapivinsky, G., Medina, I., Krapivinsky, L., Gapon, S. & Clapham, D.E. (2004) SynGAP-MUPP1-CaMKII synaptic complexes regulate p38 MAP kinase activity and NMDA receptor-dependent synaptic AMPA receptor potentiation. *Neuron*, **43**, 563–574.

Kurada, P. & White, K. (1998) Ras promotes cell survival in Drosophila by downregulating hid expression. *Cell*, **95**, 319–329.

Lee, A.C., Fenster, B.E., Ito, H., Takeda, K., Bae, N.S., Hirai, T., Yu, Z.X., Ferrans, V.J., Howard, B.H. & Finkel, T. (1999) Ras proteins induce senescence by altering the intracellular levels of reactive oxygen species. *J. Biol. Chem.*, **274**, 7936–7940.

Lin, A.W., Barradas, M., Stone, J.C., van Aelst, L., Serrano, M. & Lowe, S.W. (1998) Premature senescence involving p53 and p16 is activated in response to constitutive MEK/MAPK mitogenic signaling. *Genes Dev.*, **12**, 3008–3019.

Liu, X.B. & Jones, E.G. (1996) Localization of alpha Type II calcium/calmodulin-dependent protein kinase at glutamatergic but not gamma-aminobutyric acid (GABAergic) synapses in thalamus and cerebral cortex. *Proc. Natl Acad. Sci. USA*, **93**, 7332–7336.

Mazzoni, I.E., Said, F.A., Aloyz, R., Miller, F.D. & Kaplan, D. (1999) Ras regulates sympathetic neuron survival by suppressing the p53-mediated cell death pathway. *J. Neurosci.*, **19**, 9716–9727.

Oh, J.S., Manzerra, P. & Kennedy, M.B. (2004) Regulation of the neuron-specific Ras GTPase activating protein, synGAP, by Ca^{2+}/calmodulin-dependent protein kinase II. *J. Biol. Chem.*, **279**, 17980–17988.

Rami, A. (2003) Ischemic neuronal death in the rat hippocampus: the calpain–calpastatin–caspase hypothesis. *Neurobiol. Dis.*, **12**, 75–88.

Schweizer, C., Balsiger, S., Bluethmann, H., Mansuy, I.M., Fritschy, J.M., Mohler, H. & Luscher, B. (2003) The gamma2 subunit of GABA(A) receptors is required for maintenance of receptors at mature synapses. *Mol. Cell. Neurosci.*, **24**, 442–450.

Selkoe, D.J. (2002) Alzheimer's disease is a synaptic failure. *Science*, **298**, 789–791.

Serrano, M., Lin, A.W., McCurrach, M.E., Beach, D. & Lowe, S.W. (1997) Oncogenic ras provokes premature cell senescence associated with accumulation of p53 and p16INK4a. *Cell*, **88**, 593–602.

Sheng, M. & Sala, C. (2001) PDZ domains and the organization of supramolecular complexes. *Annu. Rev. Neurosci.*, **24**, 1–29.

Shi, Y. (2002) Mechanisms of caspase activation and inhibition during apoptosis. *Mol. Cell*, **9**, 459–470.

Stork, P.J. (2003) Does Rap1 deserve a bad Rap? *Trends Biochem. Sci.*, **28**, 267–275.

Tanaka, N., Ishihara, M., Kitagawa, M., Harada, H., Kimura, T., Matsuyama, T., Lamphier, M.S., Aizawa, S., Mak, T.W. & Taniguchi, T. (1994) Cellular commitment to oncogene-induced transformation or apoptosis is dependent on the transcription factor IRF-1. *Cell*, **77**, 829–839.

Vazquez, L.E., Chen, H.J., Sokolova, I., Knuesel, I. & Kennedy, M.B. (2004) SynGAP regulates spine formation. *J. Neurosci.*, **24**, 8862–8872.

Wang, H.G., Millan, J.A., Der Cox, A.D.C.J., Rapp, U.R., Beck, T., Zha, H. & Reed, J.C. (1995) R-Ras promotes apoptosis caused by growth factor deprivation via a Bcl-2 suppressible mechanism. *J. Cell Biol.*, **129**, 1103–1114.

Yang, J.Y. & Widmann, C. (2001) Antiapoptotic signaling generated by caspase-induced cleavage of RasGAP. *Mol. Cell. Biol.*, **16**, 5346–5358.

Yang, J.Y. & Widmann, C. (2002) The RasGAP N-terminal fragment generated by caspase cleavage protects cells in a Ras/PI3K/Akt-dependent manner that does not rely on NFkappa B activation. *J. Biol. Chem.*, **277**, 14641–14646.

Zhang, W., Vazquez, L., Apperson, M. & Kennedy, M.B. (1999) Citron binds to PSD-95 at glutamatergic synapses on inhibitory neurons in the hippocampus. *J. Neurosci.*, **19**, 96–108.